Direct Measurements of the Enthalpy of Solution of Solid Solute in Supercritical Fluids: Study on the CO_2–Naphthalene System

Xiaogang Zhang, Buxing Han,* Jianling Zhang, Hongping Li, Jun He, and Haike Yan[a]

Abstract: A setup for a calorimeter for simultaneously measuring the solubility and the solution enthalpy of solid solutes in supercritical fluids (SCFs) has been established. The enthalpy of solution of naphthalene in supercritical CO_2 was measured at 308.15 K in the pressure range from 8.0–11.0 MPa. It was found that the enthalpy of solution (ΔH) was negative in the pressure range from 8.0 to 9.5 MPa, and the absolute value decreased with increasing pressure. In this pressure range, the dissolution of the solute was enthalpy driven. However, the ΔH became positive at pressures higher than 9.5 MPa, and the dissolution was entropy driven. Monte Carlo simulation was performed to analyze the local structural environment of the solvated naphthalene molecules in supercritical CO_2 under the experimental conditions for the calorimetric measurements. By combining the enthalpy data and the simulation results, it can be deduced that the energy level of CO_2 in the high compressible region is higher than that at higher pressures, which results in the large negative enthalpy of solution and the larger degree of solvent–solute clustering in the high compressible region.

Keywords: calorimetry · carbon dioxide · naphthalene · solution enthalpy · supercritical fluids

Introduction

Recently, the thermodynamic behavior of dilute mixtures in the vicinity of the critical point of the solvent has received much attention.[1] It has been known that supercritical fluids (SCFs) have the ability to dissolve low volatile compounds; this ability is the basis of SCF techniques. The mechanism of SCFs for dissolving solutes is a very interesting and important topic, which needs to be studied further. For the supercritical (SC) CO_2–naphthalene system, solubility and partial molar volume (PMV) measurements have provided evidence that the local properties in the vicinity of the solute (naphthalene) molecules were quite different from the bulk properties of the solvent. Eckert et al.[2] proposed the idea of solvent "clustering" around the solute to interpret their experimental results of large and negative PMVs for the solutes in supercritical solvents. They showed that the infinite dilution PMV of naphthalene dissolved in CO_2 near the critical point could be predicted qualitatively by using ideal chemical theory with a cluster size of about 50 solvent molecules per solute molecule. Kim and Johnston[3] showed that the PMV of naphthalene in SC CO_2 at infinite dilution is $-7800\,cm^3\,mol^{-1}$, which corresponded to the condensation of about 80 solvent molecules around a solute molecule. They tried to combine the cluster concept with the local composition model by comparing the solubility data with solvatochromism in supercritical solutions. Debenedetti[4] compared calculations from the Kirkwood–Buff fluctuation analysis with the experimental data of Eckert et al.[2] and concluded that the cluster size was approximately 100 solvent molecules around a solute in the highly compressible region for the case of naphthalene dissolved in SC CO_2. In his analysis, it was assumed that clustering of SC solvent molecules could be related to the large negative partial molar volume. Zhong et al.[5] and Chrastil[6] proposed thermodynamic models for correlating the solubility of solutes in SCFs on the basis of clustering between solvents and solutes. The origin of the clustering in SC solutions is a very interesting question, which is closely related to the molecular interactions. The molecular interactions in SC solutions differ significantly from those in normal liquid solutions. Different experimental techniques have been used to study the molecular interactions in SCFs, such as UV,[7] FTIR,[8] fluorescence,[9] and partial molar volume measurement.[2, 10] The energy change of a given physical process could be accurately determined by using calorimetric techniques.[11] Calorimetry could provide the information about molecular interactions that cannot be obtained from other methods. Therefore, the calorimeter has been known as a "low-frequency spectrometer".[11f]

[a] Prof. B. Han, Dr. X. Zhang, Dr. J. Zhang, Dr. H. Li, Dr. J. He
Prof. H. Yan
Center for Molecular Sciences
Institute of Chemistry, the Chinese Academy of Sciences
Beijing 100080 (China)
Fax: (+86) 10-62559373)
E-mail: hanbx@pplas.icas.ac.cn

  0947-6539/01/0719-4237 $ 17.50+.50/0

The enthalpy of solution of solutes in SCFs gives energetic information about the intermolecular interactions and is a key method for investigating the reasons why SCFs are able to easily dissolve solutes. To our knowledge, however, direct measurement of the enthalpy of solution of solid solutes in SCFs has not been reported in the literature. SC CO_2–naphthalene solution has become a model system for studying solubility. This system is also a good candidate for studying structure and intermolecular interactions by experimental, theoretical, and simulation techniques. For example, recent RISM (reference interaction site model) integral equation theory calculations[12] and molecular mechanics simulations[13] have predicted the preferred orientations of CO_2 molecules around a naphthalene molecule. In this work, we established the setup for an isothermal flow calorimeter for simultaneously measuring the solubility and solution enthalpy of solid solutes in SCFs. The intermolecular interactions in the SC CO_2–naphthalene system were studied by a combination of calorimetry and Monte Carlo simulation.

Experimental Section

Materials: CO_2 with a purity of 99.995 % was supplied by Beijing Analytical Instrument Factory. Naphthalene was AR grade produced by Beijing Chemical Plant.

Supercritical calorimeter: The calorimeter was the constant temperature environment type. The principle of the calorimeter was very simple. At constant pressure, SC CO_2 flowed through a calorimeter vessel, which contained a solid solute, and dissolved the solute. The temperature of the calorimeter vessel was changed if the dissolution process absorbed or released heat. The enthalpy of solution was obtained from the mass of the solute dissolved, the energy equivalent, and the temperature change of the calorimeter vessel after correction by using graphical extrapolation based on Dickinson's method.[14]

The schematic diagram of the calorimeter is shown in Figure 1. It consisted mainly of a calorimeter vessel, an extractor (for the measuring of solubility, though strictly speaking, it did not relate to the calorimeter), a thermostat, an electric calibrator (not shown in Figure 1), a precision thermistor thermometer, a sample collector, and a high-pressure system.

The key part of the calorimeter was the calorimeter vessel, which was made of red copper and is schematically shown in Figure 2. The internal volume of the vessel was 10 mL. The outlet was a copper tube of two meters long and 1.5 mm in inner diameter and was wound around the calorimeter cell tightly so that the heat exchange was sufficient. Experiments showed that this tube was long enough because the measured enthalpy at fixed temperature and pressure was independent of the flow rate of CO_2.

Abstract in Chinese:

摘要：本文建立了同时测定溶质在超临界流体中溶解度和溶解焓的量热计，并在 308.15 K，8.0-11.0 MPa 的压力范围内测定了萘在超临界二氧化碳中的溶解焓。实验结果表明，在 8.0 到 9.5 MPa 的压力范围内，溶解焓为负，且绝对值随压力的增大而急剧变小。在此压力范围内，溶解过程为焓驱动。当压力大于 9.5 MPa 时，溶解焓变为正值，溶解过程变成熵驱动。在与实验相对应的条件下，本文还对溶液的微观结构进行了 Monte Carlo 模拟。由计算机模拟和溶解焓的实验数据推测，在低压（高度压缩区）二氧化碳分子的能位比高压区高。因此，导致高度压缩区的溶解焓为很大的负值，并使得溶质-溶剂聚集程度较大。

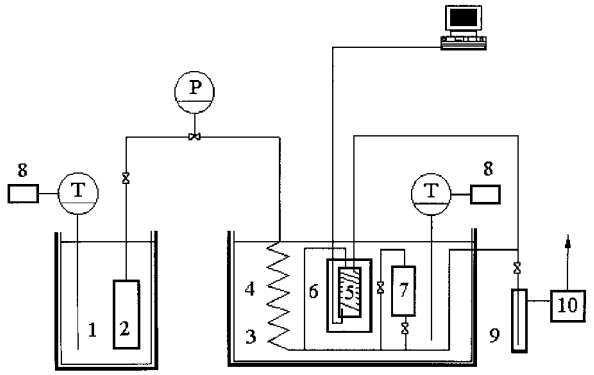

Figure 1. Schematic diagram of the calorimeter to measure solution enthalpy of solids in supercritical fluids: 1 and 3-constant temperature bath; 2-gas cylinder; 4-preheating coil; 5-calorimeter vessel; 6-outer can; 7-extractor; 8-temperature controller; 9-sample trap; 10-flow gas meter.

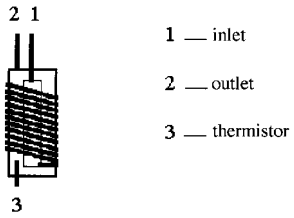

Figure 2. Schematic diagram of the calorimeter vessel.

Electrical calibration was carried out by adding power to the calibration heater with a resistance of $50 \pm 0.1\Omega$. The thermistor, which had a resistance value of 3 KΩ at 298.2 K, was sealed into the wall of the calorimeter vessel. In order to decrease the heat leaking, the surface of the calorimeter vessel, inlet and outlet tubes was electroplated, and the vessel was covered by tinfoil paper. The size of the extractor was the same as that of the calorimeter vessel, and their only difference was that the outlet of the extractor was not wound around the extractor because a long outlet was not favorable to the accurate measurement of the solubility. The accuracy of the pressure gauge, which was composed of a transducer (FOXBORO/ICT) and an indicator, was ± 0.025 MPa in the pressure range of 0–20 MPa. Temperature fluctuation of the water bath was ± 0.001 K, and the accuracy of the temperature measurement was ± 0.0005 K. The preheating coil had a length of about 15 meters. The stability of the pressure during the experiments was very important. To do this, we used a CO_2 cylinder of eight liters, which was submerged into a constant temperature water bath, as is shown in Figure 1. The pressure of the gas in the cylinder could be easily controlled by the temperature of the water bath. Experiments showed that this way was very effective because the pressure fluctuation was less than ± 0.01 MPa during each experiment.

Procedures: All the experiments were performed at 308.15 K. The calorimeter vessel and extractor were thoroughly cleaned before the experiments and then tightly packed with mixtures of solid naphthalene and copper scraps (helped to conduct heat, reduced the possibility of the solvent channeling, and prevented the solute material from forming lumps under pressure). Naphthalene (8 g) was charged for each experiment. Before the experiments, the system was stabilized for at least eight hours to reach thermal equilibrium. The solubility was determined by opening the needle valve slightly to allow CO_2 to be passed through the extractor. The solubility of the solute could be easily calculated by the masses of the solute collected and CO_2 passing through the flow meter. In order to confirm that the equilibrium inside of the extractor had been reached, the measurements were made at different flow rates (between 10 mL min^{-1} and 50 mL min^{-1}) and compared. The solubility determined was independent of the flow rate, indicating that equilibrium was reached. All the experiments were conducted at the flow rate of 30 mL min^{-1}. These data were used to calculate the mole fraction of the solute in the vapor phase at the specified

0947-6539/01/0719-4238 $ 17.50+.50/0 *Chem. Eur. J.* **2001**, *7*, No. 19

temperature and pressure. The experiments at each set of conditions were repeated at least three times, and the repeatability was better than ±2%.

The procedure for the enthalpy measurement was similar to that of the solubility measurement. CO_2 was allowed to pass through the calorimeter vessel, and the temperature change was monitored by using a computer. The mass of the solute dissolved in this process was known by the solubility under the experimental conditions and the mass of CO_2 passing through the calorimeter vessel. The energy equivalent was measured by electric calibrator under the experimental conditions, and the repeatability of the measurement was better than ±0.2%.

There was no experimental enthalpy data for the solution of solute in SCFs. However, the accuracy of the calorimeter was tested by measuring the heat capacity of water, and the average value was $4.18 \pm 0.01\ J\,g^{-1}K^{-1}$ at 308.15 K. The result agreed well with the literature value.[15] We emphasize that accuracy for the solution enthalpy of solutes in a SCF is lower than that for the heat capacity measurement of a liquid. The main reason is the uncertainty of the solubility data determined. It is estimated that the uncertainty for the enthalpy of solution determined in this work is about ±3%.

Simulation section: Monte Carlo simulation was performed on 1000 real molecules in the *NPT* ensemble with periodic boundary conditions. The *NPT* ensemble was characterized by one simulation box with the number of molecules N, pressure P, and temperature T fixed, and the volume V of the box was variable. The *NPT* ensemble was chosen instead of the canonical (Constant N, V, and T) ensemble because the latter tended to suppress density fluctuations that were important near the critical point. The molar ratios of the solvent and solute enclosed in the box were chosen in such a way that they agreed with the solubility data determined in this work. Detailed simulation conditions are given in Table 1. The standard Metropolis method was used to obtain new configurations under the *NPT* ensemble. In this work, the intermolecular potential was *Lennard–Jones* type [Eq. (1)].

$$u_{ij}(r) = 4\varepsilon_{ij}\left[\left(\frac{\sigma_{ij}}{r}\right)^{12} + \left(\frac{\sigma_{ij}}{r}\right)^{6}\right] \quad (1)$$

Table 1. Simulation conditions in the *NPT* ensemble.

Pressure [MPa]	Total Number	Naphthalene	Carbon dioxide
7.84	1000	1	999
7.92	1000	2	998
8.00	1000	3	997
8.26	1000	6	994
8.54	1000	7	993
10.15	1000	10	990
11.00	1000	10	990

In the equation, u_{ij} is the pairwise interaction. σ_{ij} and ε_{ij} are the *Lennard–Jones* size and energy parameters, and $i,j = 1,2$; 1 and 2 denote the solvent (CO_2) and the solute (naphthalene), respectively. The solute–solvent pair potential has the same form, but with different ε and σ parameters. Here we used the Lorenz–Berthelot combining rules [Eqs. (2) and (3)].

$$\varepsilon_{ij} = (\varepsilon_{ii}\varepsilon_{jj})^{1/2} \quad (2)$$

$$\sigma_{ij} = \frac{\sigma_{ii} + \sigma_{jj}}{2} \quad (3)$$

The *Lennard–Jones* parameters used in this simulation are given in Table 2. A spherical cutoff radius of the half-length of the box was taken, and the tail corrections were applied to correct for this truncation. In general, computer simulations of the mixtures near the solvent critical point can be tricky because for small finite systems different ensembles can lead to different results. We took care to make sure that in the near-critical region our results for the first peak of radial distribution functions, $g(r)$, were converged, which required large system sizes of up to 1000 particles. Regarding the equilibration issue, the first 1×10^7 MC steps were used for equilibration while the subsequent 1.1×10^7 MC steps were used for averaging of structural properties. For the *NPT* ensemble, a move involved a change in volume. The volume of the box was changed once every 100 cycles in this work. To convince ourselves that simulations were long enough, we performed separate runs starting from different configurations, including a face-centered cubic lattice and a random-distribution configuration, and obtained nearly identical results. We noted that it reached equilibration more quickly when the random-distribution configurations were adopted, thus, for each simulation, the system started from random-distribution configurations.

Table 2. Critical parameters and potential parameters for CO_2 and naphthalene.

Component	T_c [K]	P_c [MPa]	σ [Å]	ε/k [K]
carbon dioxide	304.2	7.37	3.72	236.1
naphthalene	748.4	4.05	6.45	554.4

In simulations it was often convenient to express quantities, such as temperature, density, and pressure, in reduced units. The reduced temperature, pressure, density, and length are defined as $T^* = kT/\varepsilon_{ll}$, $p^* = p\sigma^3/\varepsilon_{ll}$, $\rho^* = \rho\sigma_{ll}^3$, and $r^* = r/\sigma_{ll}$, respectively, where σ_{ll} and ε_{ll} are the parameters of the CO_2 L–J potential, T is the temperature, p is the pressure, k is the Boltzmann constant, and $\rho = N/V$ is the number density.

Results and Discussion

Enthalpy of solution: As mentioned above, the dissolution of naphthalene in SC CO_2 can reach equilibrium at the experimental conditions. Corresponding solubility data are abundant in the literature. Figure 3 compares our data with those reported in the literature.[16] The solubility data in this work are in good agreement with those determined by other authors.

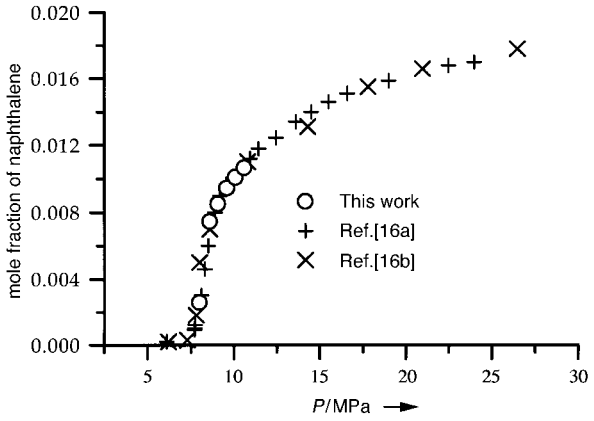

Figure 3. Comparison of the solubility data of naphthalene in supercritical CO_2 at $T = 308.15$ K determined by different authors.

Figure 3 indicates that the solubility of naphthalene in SC CO_2 is very sensitive in the pressure range of 8.0–11.0 MPa at 308.15 K, especially at pressures lower than 8.5 MPa. Our experiments focused on this pressure region.

The enthalpy of solution (ΔH) of naphthalene in SC CO_2 was measured by the calorimeter described in the Experimental Section. ΔH as a function of pressure is listed in Table 3 and is also illustrated in Figure 4. The ΔH is negative in the pressure range from 8.0 to 9.5 MPa, that is, the solution process is exothermic. The ΔH, however, becomes positive at

Table 3. Enthalpy of solution for naphthalene in SC CO_2 at 308.15 K and different pressures.

P [MPa]	ΔH [KJ mol^{-1}]
8.08	– 539.01
8.12	– 386.30
8.45	– 48.46
8.57	– 38.60
8.60	– 27.29
9.00	– 15.43
9.47	– 12.97
9.88	1.01
9.92	4.80
10.54	5.11

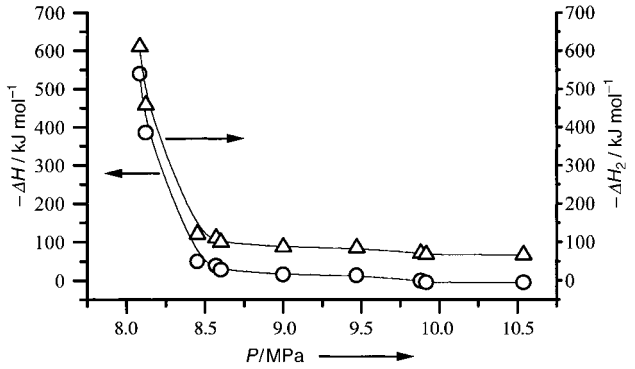

Figure 4. Dependence of solution enthalpy of naphthalene in supercritical CO_2 on pressure at $T = 308.15$ K.

the pressures higher than 9.5 MPa. ΔH increases dramatically with pressure in the range from 8.0 to 8.5 MPa.

The Gibbs free energy (ΔG), enthalpy (ΔH), and entropy (ΔS) of solution are related by the following well-known Equation (4).

$$\Delta G = \Delta H - T\Delta S \tag{4}$$

Increasing ΔH is not favorable to increasing the solubility, while an increase in ΔS is favorable to the solubility increase. In the high compressible region, solution enthalpy is a large negative value, that is, the enthalpy effects are dominant for the dissolution of the solute. ΔH increases with increasing pressure and becomes positive at the higher pressures. At these pressures, the solution entropy must be large enough to dissolve the solute in the supercritical fluid. In other words, the entropy effects become dominant for the dissolution of the solid at higher pressures. ΔH can be divided into two parts [Eq. (5)].

$$\Delta H = \Delta H_1 + \Delta H_2 \tag{5}$$

ΔH_1 is the enthalpy of sublimation of naphthalene in the absence of CO_2. ΔH_2 is the enthalpy of solution for dissolving gaseous naphthalene in SC CO_2 and gives energetic information on the intermolecular interactions. The effect of static pressure on ΔH_1 should not be considerable in the pressure range studied in this work. The value of ΔH_1 is 71.27 KJ mol^{-1}.[17] The ΔH_2 was easily obtained from Equation (5), and the results are also shown in Figure 4. As expected, ΔH_2 is negative over the entire pressure range studied, and the absolute value decreases with increasing pressure. We will discuss this further after discussion of the microstructure of the solution.

Microstructure of the naphthalene/CO_2 solution: In order to understand the molecular interactions of naphthalene – CO_2 and analyze the above experimental results, we used the *NPT* Monte Carlo method to study the microstructure of the solution under some typical conditions for the enthalpy experiments. The molar ratios of the two components enclosed in the box were corresponding to the solubility determined in this work. Thus we can discuss the intermolecular interactions by combination of the simulation results and the calorimetric data.

The radial distribution function (RDF) gives the probability of finding a pair of particles at a distance r apart, relative to the probability expected for a completely random distribution at the same density. Any deviation of RDF from unity reflects the correlation between the particles due to the intermolecular interactions. It provides information about the local fluid structure. Figure 5 shows the RDFs in CO_2 – naphthalene systems at 308.15 K. The parameter $g_{11}(r)$ is the

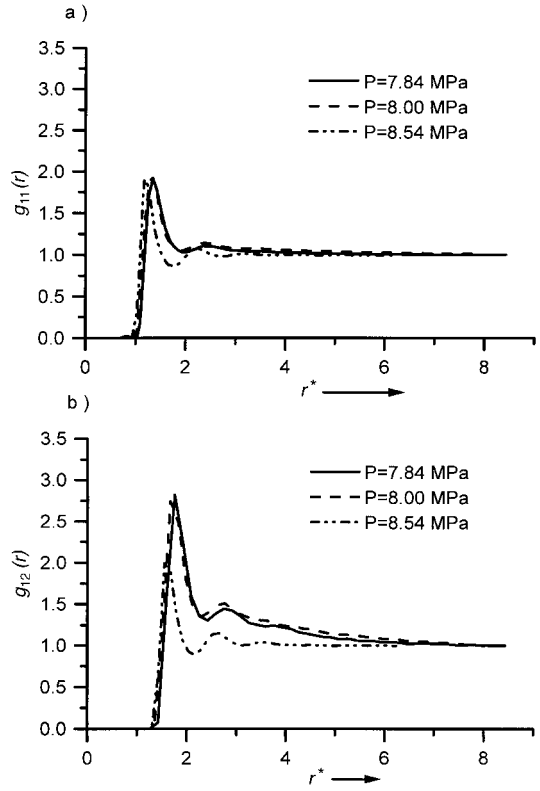

Figure 5. The RDFs of CO_2 – CO_2: a) and CO_2 – naphthalene; b) at 308.15 K and different pressures.

RDF of the CO_2 – CO_2 pair, and $g_{12}(r)$ stands for the RDF of the CO_2 – naphthalene pair. In $g_{11}(r)$, the oscillation structure tends to disappear from high pressure to critical pressure, while in $g_{12}(r)$, the short-range (first peaks) and long-range correlations increase near the critical state. The figure, furthermore, indicates that the first peak $g_{12}(r)$ is higher than

0947-6539/01/0719-4240 $ 17.50+.50/0 *Chem. Eur. J.* **2001**, *7*, No. 19

that of $g_{11}(r)$ in the critical state, that is, there is preferential aggregation of CO_2 about the naphthalene solute. In the high-pressure region, however, the heights of the first peak of $g_{12}(r)$ and $g_{11}(r)$ are almost the same, and strong correlations between solvent and solute disappear. It implies that the enhancement of local density due to the presence of the attractive naphthalene solute is more pronounced when the fluid is more compressible. Such a trend was also observed in Nouacer and Shing's simulation study for infinitely dilute solution.[18]

Extensive experimental and theoretical studies of dilute supercritical solutions have shown that the local environment around a dilute solute can differ dramatically from that around a solvent molecule.[19] A cluster is a simple and practical concept to explain a variety of phenomena in supercritical fluids. However, one should be aware that the term "cluster" does not imply the existence of stable physical aggregation. An important feature of a supercritical fluid is the large fluctuation in its density both over space and time, which may control the phenomena occurring in the supercritical state, particularly near the critical point. In this work, we try to use the concept of "clustering" to explain the phenomena of our measurements.

Debenedetti[4] and Kim and Johnston[20] defined the mean cluster size of solvent molecules about a solute molecule in dilute solution as in Equation (6).

$$\xi_{12} = 4\pi\rho_1 \int [g_{12}(r) - 1] r^2 dr \tag{6}$$

In the equation, ρ_1 is the number density of the solvent. In the same way, the mean cluster size between solvents could be defined in Equation (7).

$$\xi_{11} = 4\pi\rho_1 \int [g_{11}(r) - 1] r^2 dr \tag{7}$$

According to Equations (6) and (7), we computed the cluster size of CO_2-CO_2 and naphthalene$-CO_2$ in naphthalene$-CO_2$ systems, and of CO_2-CO_2 in pure CO_2, respectively. The calculations were carried out at some typical conditions for enthalpy measurements. From Figure 6, we can see that both the cluster size of naphthalene$-CO_2$ and CO_2-CO_2 reached a maximum in the high compressible region. Furthermore, the cluster size of CO_2-CO_2 in the naphthalene$-CO_2$ system is similar to that in pure CO_2 in the pressure range, which implies that under our experimental conditions,

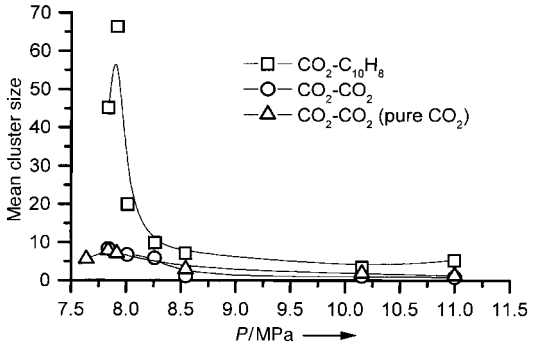

Figure 6. Mean cluster size of CO_2-CO_2 and CO_2-naphthalene in the CO_2-naphthalene system and in pure CO_2.

the addition of attractive solute into the solvent does not considerably change the aggregation of solvent molecules themselves.

Figure 4 shows that the enthalpy change (ΔH_2) is negative when gaseous naphthalene is added to SC CO_2. The absolute value decreases sharply with pressure in the pressure range from 8.0 to 8.5 MPa and decreases slowly with pressure at higher pressures. By combining the results in Figure 6, it can be concluded that the ΔH_2 is closely related with the clustering of CO_2 about the solute naphthalene.

It should be emphasized that the cluster size calculated from Equations (6) and (7) is the average number of CO_2 molecules in each cluster in excess of the number expected in that volume on the basis of the bulk density, and these results give a clear picture of the clustering of CO_2 surrounding the solute. However, to study the molecular interactions, we should calculate the total coordination number $n_{ij}(r)$ of CO_2 around the solute. Based on Equations (6) and (7), it can be easily calculated from the following Equation (8).

$$n_{ij}(r) = 4\pi\rho_j \int_0^r g_{ij}(r) r^2 dr \tag{8}$$

The coordination number of CO_2 about a solute as a function of r is listed in Table 4. The $n_{12}(r)$ increase with pressure for all r values.

Table 4. Coordination number of CO_2-naphthalene in different solvation shells.

P [MPa]	n_{12} [r = 7.4 Å]	n_{12} [r = 11.2 Å]	n_{12} [r = 14.9 Å]	n_{12} [r = 18.6 Å]
7.92	11.91	40.90	101.53	180.45
8.26	12.50	46.63	112.52	204.62
8.54	14.69	51.85	121.40	233.28
9.26	13.41	50.83	124.03	245.51
10.15	16.50	57.80	135.88	263.05
11.00	16.61	58.60	138.29	268.43

As discussed above, the effect of naphthalene on the interactions between CO_2 in the bulk solution can be neglected. For a first approximation, ΔH_2 can be considered as the enthalpy change for the clustering process of one mole of gaseous naphthalene with CO_2. There are two possible reasons for the large negative value of ΔH_2 in the high compressible region. First, the interaction between the solvent and solute is stronger. Second, the energy level of the CO_2 at lower pressures (high compressible region) is higher than that at higher pressures, and thus more heat is given out when it forms the solvent–solute clusters. We cannot find the evidence to support the first assumption. It can be assumed that the coordination number of solvent molecules around the solute is larger if the interaction between the solvent and solute is stronger. The results in Table 4 show that the coordination number of CO_2 molecules around the solute increases with increasing pressure. Thus, we can deduce that the energy level of the CO_2 in the high compressible region is higher than that at higher pressures, and thus more heat is given out when it forms solvent–solute clusters. This in turn can explain why the degree of clustering is larger in the higher compressible region.

Acknowledgements

This work was financially supported by the National Natural Science Foundation of China (29725308), National Key Basic Research Project (G2000048010), the Chinese Academy of Sciences, and the Royal Society. The authors are very grateful to Professor M. Poliakoff for the valuable suggestions.

[1] a) O. Kajimoto, *Chem. Rev.* **1999**, *99*, 355 – 389; b) S. A. Egorov, *J. Chem. Phys.* **2000**, *112*, 7138 – 7146; c) S. A. Egorov, *J. Chem. Phys.* **2000**, *113*, 1950 – 1957; d) S. A. Egorov, A. Yethiraj, J. L. Skinner, *Chem. Phys. Lett.* **2000**, *317*, 558 – 566.

[2] a) C. A. Eckert, D. H. Ziger, K. P. Johnston, T. K. Elison, *Fluid Phase Equilib.* **1983**, *14*, 167 – 175; b) C. A. Eckert, D. H. Ziger, K. P. Johnston, S. Kim, *J. Phys. Chem.* **1986**, *90*, 2738 – 2746; c) C. A. Eckert, B. L. Knutson, P. G. Debenedetti, *Nature* **1996**, *383*, 313 – 318.

[3] S. Kim, K. P. Johnston, *AIChE J.* **1987**, *33*, 1603 – 1611.

[4] P. G. Debenedetti, *Chem. Eng. Sci.* **1987**, *42*, 2203 – 2221.

[5] M. Zhong, B. Han, J. Ke, H. Yan, D. Peng, *Fluid Phase Equilib.* **1998**, *146*, 93 – 100.

[6] J. Chrastil, *J. Phys. Chem.* **1982**, *86*, 3016 – 3027.

[7] a) Y. P. Sun, M. A. Fox, K. P. Johnston, *J. Am. Chem. Soc.* **1992**, *114*, 1187 – 1194; b) J. Zhang, D. R. Roek, J. E. Chateauneuf, J. F. Brennecke, *J. Am. Chem. Soc.* **1997**, *119*, 9980 – 9989; c) J. Lu, B. Han, H. Yan, *Ber. Bunsen-Ges.* **1998**, *102*, 695 – 700.

[8] a) N. Wada, M. Saito, D. Kitada, *J. Phys. Chem. B* **1997**, *101*, 10918 – 10926; b) J. Ke, S. Jin, H. Yan, *J. Supercrit. Fluids* **1997**, *11*, 53 – 65.

[9] a) J. F. Brennecke, D. L. Tomasko, C. A. Eckert, *J. Phys. Chem.* **1990**, *94,* 7692 – 7702; b) Y. P. Sun, G. Bennett, K. P. Johnston, *J. Phys. Chem.* **1992**, *96*, 10001 – 10016.

[10] M. Zhong, J. Ke, B. Han, H. Yan, *Acta Physico-chimica Sinica* **1996**, *12*, 816 – 829.

[11] a) I. Wadsö, *Thermochim. Acta* **1995**, *250*, 285 – 304; b) M. J. Dauncey, *Thermochim. Acta* **1991**, *193*, 1 – 40; c) A. E. Beezer, *Thermochim. Acta* **1995**, *250*, 277 – 283; d) A. Blume, *Thermochim. Acta* **1991**, *193*, 299 – 347; e) L. D. Hansen, *Pure Appl. Chem.* **1998**, *7*, 687 – 694; f) R. Stanislawl, *Recent Developments in Calorimetry. Annual Reports on the Progress of Chemistry, Physical Chemistry, Vol. 94 Section C*, Royal Society of Chemistry, Cambridge, **1998**, pp. 433 – 491; g) P. R. Murthy, J. D. Moore, A. C. Lewellen, *J. Chem. Thermodyn.* **1996**, *28*, 363 – 371.

[12] K. Koga, H. Tanaka, X. Zeng, *J. Phys. Chem.* **1996**, *100*, 16711 – 16719.

[13] P. Battersby, *J. Comput. Chem.* **1994**, *15*, 580 – 587.

[14] H. C. Dickinson, *Bull. Natl. Bur. Stand.* **1914**, *11*, 189 – 193.

[15] *CRC Handbook of Chemistry and Physics* (Ed.: R. C. Weast), CRC Press, Boca Raton, **1985 – 1986**, pp. D-171.

[16] a) Y. Tsekhanskaya, M. Iomtev, E. Mushkina, *Russ. J. Phys. Chem.* **1964**, *9*, 1173 – 1186; b) S. T. Chung, K. S. Shing, *Fluid Phase Equilib.* **1992**, *81*, 321 – 332.

[17] G. C. Najour, A. D. King, Jr., *J. Chem. Phys.* **1966**, *45*, 1915 – 1921.

[18] M. Nouacer, K. S. Shing, *Mol. Simul.* **1989**, *2*, 55 – 69.

[19] a) O. Kajimoto, M. Futakami, T. Kobayashi, K. Yamasaki, *J. Phys. Chem.* **1988**, *92*, 1347 – 1352; b) J. F. Brennecke, D. L. Tomasko, J. Peshkin, C. A. Eckert, *Ind. Eng. Chem. Res.* **1990**, *29*, 1682 – 1699; c) C. Carlier, T. W. Randolph, *AIChE J.* **1993**, *39*, 876 – 889; d) J. Zhang, L. L. Lee, J. F. Brennecke, *J. Phys. Chem.* **1995**, *99*, 9268 – 9274; e) P. B. Baulbuena, K. P. Johnston, P. J. Rossky, *J. Am. Chem. Soc.* **1994**, *116*, 2689 – 2690; f) J. Zagrobelny, T. A. Betts, F. V. Bright, *J. Am. Chem. Soc.* **1992**, *114*, 5249 – 5259; g) J. Zagrobelny, F. V. Bright, *J. Am. Chem. Soc.* **1992**, *114,* 7821 – 7826; h) K. Takahasi, K. Abe, S. Sawamura, C. D. Jonah, *Chem. Phys. Lett.* **1998**, *282*, 361 – 366.

[20] S. Kim, K. P. Johnston, *Ind. Eng. Chem. Res.* **1987**, *26*, 1206 – 1215.

Received: April 17, 2001 [F3200]

  0947-6539/01/0719-4242 $ 17.50+.50/0